The Journal of Chemical Physics ARTICLE scitation.org/journal/jcp

Catalysis on oxidized ferroelectric surfaces—Epitaxially strained $LaTiO_2N$ and $BaTiO_3$ for photocatalytic water splitting

Cite as: J. Chem. Phys. 152, 024701 (2020); doi: 10.1063/1.5135751
Submitted: 8 November 2019 • Accepted: 13 December 2019 •
Published Online: 8 January 2020

Nathalie Vonrüti and Ulrich Aschauer[a)]

AFFILIATIONS

Department of Chemistry and Biochemistry, University of Bern, Freiestrasse 3, CH-3012 Bern, Switzerland

Note: This article is part of the JCP Special Topic on Oxide Chemistry and Catalysis.
[a)]**Email:** ulrich.aschauer@dcb.unibe.ch

ABSTRACT

Surface properties of ferroelectrics are promising for catalysis due to the spontaneous electric polarization that can be reversed by an applied electric field. While several theoretical studies show different catalytic activities for differently polarized ferroelectric surfaces at zero electric potential, little work was devoted to catalysis on ferroelectric surfaces at higher electric potentials. Under these conditions that are relevant for photocatalytic experiments and applications, surfaces are usually oxidized. Using density functional theory calculations, we show for $LaTiO_2N$ and $BaTiO_3$ that this oxidation heavily impacts and even determines the electronic properties of the catalyst surface and therefore leads to similar reaction free energies for the catalytic steps of the oxygen evolution reaction, irrespective of the bulk polarization. This is opposed to experimental studies, which found different activities for differently polarized catalyst surface domains under oxidizing conditions. We therefore conclude that the experimentally observed activity difference does not originate from the surface polarization following the bulk polarization, but rather from different bulk polarization directions leading to different adsorbate coverages or even surface reconstructions.

I. INTRODUCTION

Ferroelectrics have been investigated as catalyst materials for several decades due to their interesting surface properties that could pave the way toward dynamic surface catalysis, where the catalytic properties are actively changed as a function of time. Ferroelectrics are materials that show a spontaneous electric polarization $\vec{P}$ that can be reversed by the application of an external electric field. The internal electric polarization $\vec{P}$ of ferroelectrics would induce a large depolarizing field $\vec{E}$ in the opposite direction. Therefore, electrons move from the negatively polarized end of the material to the positively polarized end, while holes move in the opposite direction, canceling the electric field. This preferential migration leads to an improved electron-hole separation and a hole electron doped surface,[1–3] respectively (see Fig. 1). In fact, it was shown that oxidation and reduction processes preferably happen on negatively and positively polarized domains, respectively.[4,5] Furthermore, by applying an electric field, one could possibly switch between these two differently doped surfaces, thus providing a way to achieve dynamic surface properties and to go beyond the limits of the Sabatier principle.[6–8] This principle states that the optimum catalytic activity of a fixed surface is limited by an intermediate bond strength between the adsorbate and the catalyst: While the bond strength between the reactant and the catalyst should be as strong as possible, the bond strength between the product and the surface should be as weak as possible. This compromise leads to a maximum catalytic activity[9,10] and is often represented graphically in the so-called volcano plot.[11]

Theoretical studies so far only investigated the influence of the ferroelectric polarization on the catalytic properties of surfaces without oxidizing adsorbates.[1,12,13] In (photo)catalysis, surfaces are, however, often oxidized when operated under a positive potential. While an effect of the bulk polarization on the catalytic activity was experimentally reported under conditions

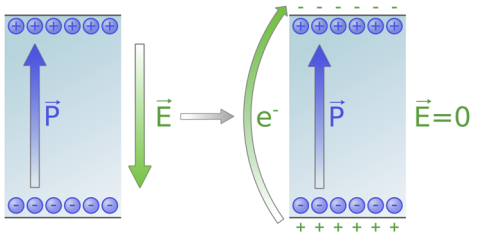

FIG. 1. Schematic of electronic reconstructions in ferroelectrics: ferroelectrics have an internal electric polarization $\vec{P}$, which leads to a depolarizing field $\vec{E}$ that acts to neutralize $\vec{P}$. As a result, electrons and holes move to oppositely polarized surfaces, canceling $\vec{E}$ and creating an electron and hole doped surface, respectively.

that should lead to surface oxidation,[5] there are, to the best of our knowledge, neither theoretical nor experimental studies on the underlying mechanism or on the electronic and atomic structure of oppositely polarized ferroelectric surfaces under application conditions.

We therefore investigate here, using density functional theory (DFT) calculations, the effect of the polarization of clean and oxidized ferroelectric surfaces on the oxygen evolution reaction (OER). We study these processes using an epitaxially strained and, hence, ferroelectric oxynitride[14–16] $LaTiO_2N$[17] and the prototypical ferroelectric $BaTiO_3$ as catalyst materials. Oxynitrides were shown to be promising photocatalysts for solar water splitting[18,19] due to their small bandgap and the positions of the valence and conduction band edges that straddle the oxygen and hydrogen evolution potential, respectively. The rate limiting reaction of the overall water-splitting reaction is the OER, which involves photogenerated holes and occurs under oxidizing conditions—normally leading to surface oxidation of the photocatalyst. This is also the case for oxynitrides for which the valence band (VB) maximum lies around 2 V below the standard hydrogen electrode (SHE).[20] Even though $BaTiO_3$ has a bandgap of 3.2 eV[21] which is too large for visible-light photocatalysis, it is well suited for comparison with the ferroelectric oxynitride since (as opposed to the oxynitride) its performance as a ferroelectric photocatalyst was experimentally studied under oxidizing conditions.[3,5]

We first analyze the electronic properties of the clean surfaces and the effect of the ferroelectric polarization on the OER of compressively strained $LaTiO_2N$. Subsequently, we investigate how the electronic properties and OER energetics change when the surface is oxidized. While we find for the clean surface a clear difference in the electronic structure and hence OER activity for the opposite polarization, these differences vanish when the surface is oxidized, leading to virtually the same OER energetics for oppositely polarized domains. To confirm that our observations are valid also for more established ferroelectrics, we show similar findings for $BaTiO_3$ in Secs. S2–S4 of the supplementary material.

II. COMPUTATIONAL DETAILS

DFT calculations were performed with Quantum ESPRESSO[22] at the PBE+U level of theory.[23,24] All atoms are represented by ultrasoft pseudopotentials[25] with Ba(5s, 5p, 5d, 6s, 6p), La(5s, 5p, 5d, 6s), Ti(3s, 3p, 3d, 4s), O(2s, 2p), N(2s, 2p), and Pt(6s, 5d) as valence electrons. A Hubbard U of 3.0 eV was applied to the Ti 3d orbitals as in our previous studies.[17,26] The cutoff for the plane wave basis set was 40 Ry for the kinetic energy combined with 320 Ry for the augmented density.

For $LaTiO_2N$, we start our calculations from a ferroelectric 40-atom pseudocubic perovskite cell with a *trans* anion order where the Ti–N bonds form 180° angles (see Fig. 2). We obtained this structure in our previous work[17] by straining $LaTiO_2N$ epitaxially by −4%. The *trans* anion order results in alternating charge-neutral TiO_2 and LaN atomic layers. We then create asymmetric 1 × 1 × 2 (001) surface slabs with at least 10 Å vacuum and the direction of the ferroelectric displacement parallel to the surface normal. Tests on larger cell sizes showed that this system size is adequate for our purposes (see Secs. S4–S6 of the supplementary material). We will refer to a *positively polarized bulk* when the positive end of the electric polarization vector points toward the surface and a *negatively polarized bulk* when the negative end of the polarization vector points toward the surface. We restrict ourselves to the investigation of the B-terminated (TiO_2) surface, which we found to be

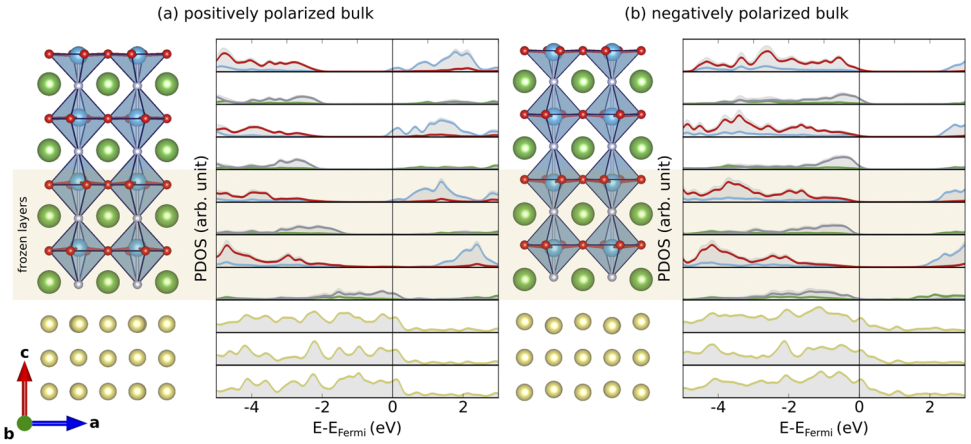

FIG. 2. Atomic structure and layer-resolved partial density of states (PDOS) of the *trans* $LaTiO_2N$ (001) surface with (a) positively polarized bulk resulting in an electron doped surface and (b) negatively polarized bulk resulting in a hole doped surface. Color code: La = green, Ti = blue, O = red, N = gray, and Pt = yellow.

thermodynamically more stable for $LaTiO_2N$.[27] We fix four atomic layers at the bottom to simulate the bulk material and also add three layers of platinum at the bottom of the slab. The addition of the platinum layers is a standard procedure when simulating ferroelectric surfaces as they represent an electron reservoir that exists in thick ferroelectric films.[7,12] To avoid spurious energy contributions, these Pt atoms were allowed to relax only for the clean surface but kept fixed at these relaxed positions in all calculations with adsorbates. We also add a dipole correction[28] to cancel the spurious electric field across the vacuum gap. The Brillouin zone is sampled with $4 \times 4 \times 4$ and $4 \times 4 \times 1$ Monkhorst-Pack k-point grids[29] for the bulk and surface slab, respectively. The convergence criteria for geometry relaxations were 0.05 eV/Å for forces and 1.4×10^{-5} eV for the total energy. Small deviations in the computational setup for the $BaTiO_3$ calculations can be found in Sec. S2 of the supplementary material. Atomic structures were visualized using VESTA.[30]

We calculate reaction free energies of the OER steps via differences (ΔE_{ads}) in adsorption energies (E_{ads}) of the different intermediates at a given pH and potential U_{SHE} with respect to the standard hydrogen electrode (SHE) as follows:[31]

$$\Delta G_{ads} = \Delta E_{ads}^{DFT} - T\Delta S + \Delta ZPE - neU_{SHE} - hkT\ln(10)pH, \quad (1)$$

where ZPE is the zero-point energy, S is the entropy, and n and h represent the number of electrons and protons, respectively. Values for ZPE and S were taken from elsewhere,[32] and the temperature was chosen to be at standard conditions (T = 298.15 K). Similarly, we can calculate the shift of the valence band (VB) maximum with pH according to the Nernst equation as follows:

$$V_{VB}(pH) = V_{VB}(0) - kT\ln(10)pH. \quad (2)$$

In electrochemistry, the rate determining step ΔG_{max} of a reaction minus the equilibrium potential ΔG_0 (ΔG_0^{OER} = 1.23 V) to drive the reaction is referred to as the overpotential η,

$$\eta = \frac{\Delta G_{max}}{e} - \Delta G_0. \quad (3)$$

As the overpotential is independent of the applied potential and pH, we calculate all differences in adsorption energies at standard conditions where the potential and pH are zero. To circumvent the cumbersome calculation of solvated ionic species e^- and H^+ within DFT, we use the computational standard hydrogen electrode from the work of Nørskov *et al.*,[31] where the energy of $H^+ + e^-$ is equal to the energy of half a H_2 molecule. Furthermore, we approximate the energy of the O_2 molecule [which is not well described by the local-density approximation (LDA) or generalized gradient approximation (GGA)[33]] by assuming that the overall water splitting reaction requires the experimental energy difference of 4.92 eV (four times the equilibrium potential ΔG_0 times e), resulting in

$$E_{O_2} = 4.92\ eV - 2E_{H_2} + 2E_{H_2O} - (\Delta ZPE - T\Delta S)_{2H_2O} \rightarrow O_2 + 2H_2 \quad (4)$$

for the O_2 energy.

III. RESULTS AND DISCUSSION

We start our analysis by investigating the electronic structure of the surfaces with oppositely polarized bulk in $LaTiO_2N$. We do so by analyzing the layer-resolved partial density of states (PDOS). In agreement with our simple picture of the electronic compensation of the ferroelectric polarization (see Fig. 1) and other studies,[1,13] we see that while the surface of the positively polarized bulk is electron doped [Fermi energy in the conduction band on the surface layer, see Fig. 2(a)], the surface of the negatively polarized bulk is hole doped [Fermi energy in the valence band on the surface layer, see Fig. 2(b)]. By looking at the atomic surface structure, we can further see that for the positively polarized bulk, the first unit cell that is allowed to relax has the same polarization direction as the bulk but a slightly smaller distortion amplitude. In the topmost unit-cell, however, the polarization direction is reversed. For the structure with the negatively polarized bulk, all atomic layers keep the same polarization direction as the bulk. We can explain the change in polarization of the topmost atomic layers for the positively polarized bulk structure by the under-coordination of the titanium cations that prefer a stronger bond with the underlying nitrogen ions.

We continue by analyzing the OER on surfaces of the two oppositely polarized bulk structures for which we find very different free energy profiles. For the OER, we consider the conventional mechanism that proceeds on transition-metal sites and consists of four consecutive proton-coupled one-electron transfer (PCET) steps with reaction intermediates *OH, *O, and *OOH, as shown in the following equations (see also the structures at the bottom of Fig. 3):

$$* + H_2O(l) \rightarrow *OH + H^+ + e^-, \quad (5)$$

$$*OH \rightarrow *O + H^+ + e^-, \quad (6)$$

$$*O + H_2O(l) \rightarrow *OOH + H^+ + e^-, \quad (7)$$

$$*OOH \rightarrow * + O_2(g) + H^+ + e^-, \quad (8)$$

where $*$ denotes the reactive site on the surface. The reaction is endothermic and requires an energy of 4.92 eV. Ideally, each of

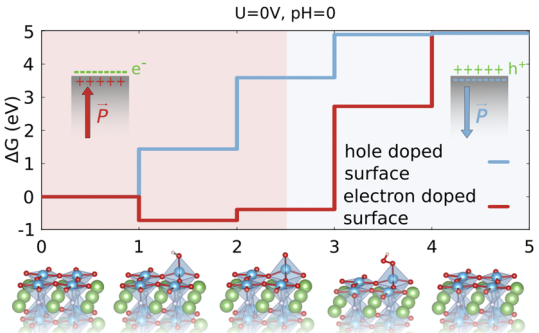

FIG. 3. Free energy profile for the OER on the (red) electron and (blue) hole doped *trans* $LaTiO_2N$ (001) surface at a potential of 0 V and at pH 0. The red and the blue background colors indicate the regions where the electron doped and hole doped surfaces, respectively, lead to smaller free energy steps. At the bottom, the different reaction intermediates adsorbed on the surface are depicted. Color code: La = green, Ti = blue, O = red, N = gray, and H = white.

the four electrochemical steps would therefore require a potential of 1.23 V. However, due to the so-called universal scaling relations that impose a constant difference of 3.2 eV between the OOH and OH adsorption energies (which would ideally have an energy difference of only 2 · 1.23 eV), the theoretical minimum overpotential for the OER, proceeding via these four PCET steps, is $0.37\,\mathrm{V} = \frac{1}{2}(3.2\,\mathrm{V} - 2 \cdot 1.23\,\mathrm{V})$.[11]

In Fig. 3, we show the free energy profile of the OER on the nonoxidized surface for the two opposite polarization directions of the bulk. We find that due to a charge transfer between the surface and the adsorbate, for the positively polarized bulk (i.e., electron doped surface), the steps involving a surface oxidation (i.e., steps 1 and 2) have small or even negative free energy changes, while the steps involving a surface reduction (i.e., steps 3 and 4) have larger free energy changes. The opposite is true for the negatively polarized bulk (i.e., hole doped surface) where the surface oxidation steps are larger (i.e., steps 1 and 2) compared to the surface reduction steps (i.e., steps 3 and 4). These results agree well with other theoretical studies on free energy changes on surfaces with oppositely polarized bulk structures.[1,12,13] Furthermore, these results suggest that ferroelectric $LaTiO_2N$ could overcome the Sabatier principle by changing the polarization direction from a positively polarized to a negatively polarized bulk between steps 2 and 3 by applying an electric field. In this way, the largest step of the free energy diagram is 1.31 eV, representing an overpotential of only 0.08 eV, which is much smaller than the theoretical minimum overpotential of 0.37 V predicted by the universal scaling relations.[11]

Under a positive electrochemical potential, the surface is normally oxidized (e.g., surface passivation or surface corrosion). To determine surface structures under these conditions, we calculate the surface phase diagram of the H_2O + $LaTiO_2N$ surface system as a function of the potential at pH 11 for the negatively and positively polarized bulk (see Fig. 4). To do so, we calculate DFT energies of the polarized $LaTiO_2N$ slabs that are fully covered with hydroxo and oxygen adsorbates, respectively (one adsorbate attached to each transition metal). The potential of a photocatalyst is determined by the energy difference between the valence band edge and the SHE, which for $LaTiO_2N$ is between 2 V[20] and 1.2 V for a pH between 0 and 14. At this potential, the surfaces of both the positively and negatively polarized bulk are covered by oxygen adsorbates at pH 11 (see Fig. 4) and by hydroxo species at pH 0 (see Fig. S1 of the supplementary material). While in reality a mixture of hydroxo and oxygen species could be present, we tested here, for simplicity, only surfaces covered fully with either hydroxo or oxygen adsorbates. We see that the positively charged surface (negatively polarized bulk) gets oxidized at higher potentials than the negatively charged surface (positively polarized bulk). We can explain this by an electron transfer similar to the case of the nonoxidized surfaces, where the electrons move to the surface of the positively polarized bulk and the holes to the surface of the negatively polarized bulk. The electron-doped surface of the positively polarized bulk then facilitates the adsorption of more electronegative neutral atomic species and therefore leads to a surface oxidation at lower potentials compared to the negatively polarized bulk.

Comparing the layer-resolved PDOS of the oxidized surfaces with negatively and positively polarized bulk structures, we find that both surfaces are hole doped due to an electron depletion at the surface as a result of the oxygen adsorbates (see Fig. 5). Moreover, the surface oxidation leads to large structural changes in the surface layers—especially for the negatively polarized bulk, where the direction of the atomic displacements in the four topmost atomic layers (the ones without fixed atomic positions) is inverted. We can rationalize this finding by the fact that for the negatively polarized bulk, the negative bound charge at the clean surface is compensated by holes. The adsorption of O or OH species, however, relies on an electron transfer from the surface to the adsorbate. Inverting the polarization at the surface of the slab with the negatively polarized bulk makes these electrons available but also leads to the formation of a ferroelectric domain wall associated with an energy penalty. For our thin slab, the position of this wall has to be between the frozen and free layers, but in films or nanoparticles, we expect a thicker surface domain to form, our model thus having the domain wall spuriously close to the surface. This view is further supported by the fact that the polar displacement amplitude in the presence of adsorbates is much larger than without, which correlates with the availability of electrons needed for adsorption on the surface.

We now compute the OER on oxidized surfaces and find that due to the electron depletion of the surface caused by the oxidizing adsorbates, the effect of the bulk polarization on the OER is almost negligible. Figures 6(a) and 6(b) show the free energy differences of the OER reaction steps on the surface covered with hydroxo and oxygen, respectively. For the hydroxo covered surface, the OER is almost identical irrespective of the bulk polarization. For the oxygen

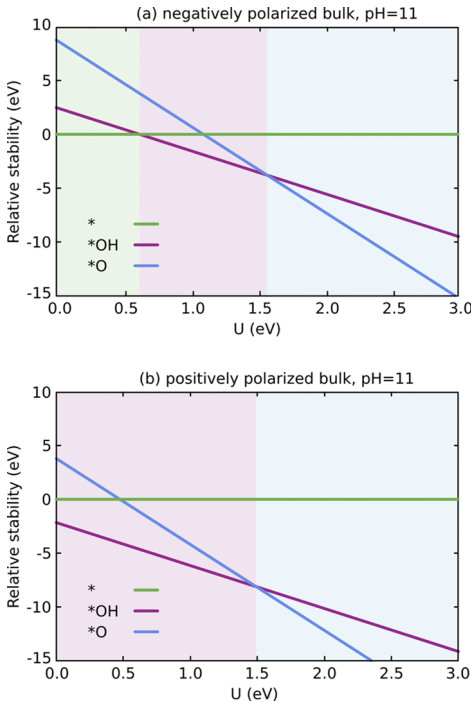

FIG. 4. Phase diagram of the H_2O + *trans* $LaTiO_2N$ (001) surface calculated as a function of the potential at pH 11 for (a) the negatively polarized bulk and (b) the positively polarized bulk.

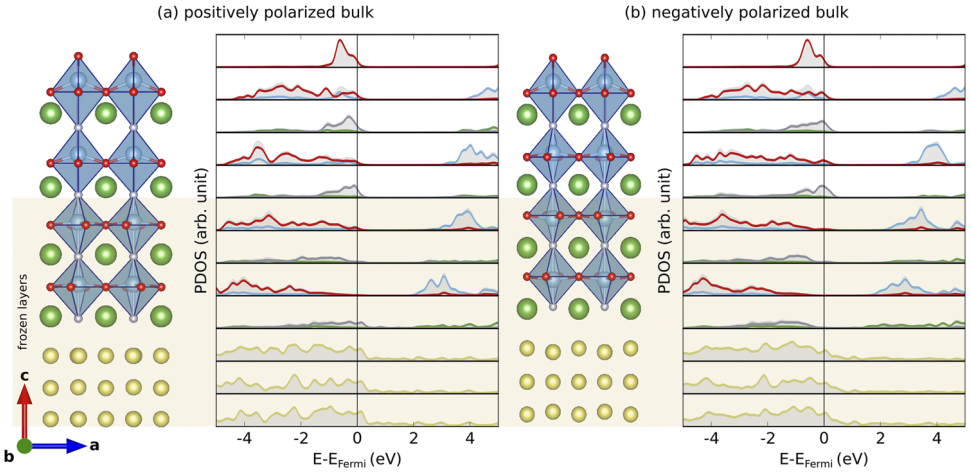

FIG. 5. Atomic structure and layer-resolved partial density of states (PDOS) of the oxidized *trans* $LaTiO_2N$ (001) surface with (a) positively polarized bulk resulting in a hole doped surface and (b) negatively polarized bulk also resulting in a hole doped surface. Color code: La = green, Ti = blue, O = red, N = gray, and Pt = yellow.

covered surface also, most of the step energies are identical except for the steps involving the peroxo (*OOH) intermediate. This difference between the two polarization directions is, however, not directly caused by the bulk polarization but by the decay of the peroxo species into two different fragments for the positively and negatively polarized bulk, respectively [see the inset of Fig. 6(b)]. We cannot exclude that this decay originates from the presence of the domain wall for the negatively polarized bulk and therefore indirectly from the bulk polarization, which would require an extensive investigation of the OER on much thicker slabs. The decay could, however, also be due to slightly different starting coordinates for the relaxations. The occurrence of two different reaction mechanisms would, therefore, require an in-depth analysis of alternative reaction mechanisms, based on adsorption energies of different reaction intermediates. We do, however, believe that the effect of the domain wall and the correct reaction mechanism are secondary for this investigation, as the surface oxidation leads to an almost identical surface electronic structure and should therefore also result in similar reaction mechanisms and hence similar free energy differences for the two oppositely polarized bulk structures for much thicker slabs.

The above results imply that the effect of the bulk polarization on the free energy differences of the OER steps completely vanishes when the surface polarization is reversed due to oxidizing adsorbates. The observed interaction between surface adsorbates and the ferroelectric state was previously named "ferroionics"[34] and is supported by multiple experimental findings. As such, it was shown for ultrathin $PbTiO_3$ films that the polarization direction can affect the surface chemistry and that the chemical environment can also change the polarization direction of the thin film.[35] Recently, it was shown that the bulk polarization in $BiFeO_3$ films below 60 nm thickness can be switched by tuning the H^+/OH^- concentration in aqueous solution.[36] Finally, for $BaTiO_3$, it was shown that the polarization of the surface layer was pinned when exposed to water and only the bulk part is switchable by an electric field.[37]

Our findings and these previously published results, however, contradict the experimentally reported different catalytic activities for differently polarized ferroelectric domains of $BaTiO_3$,[3,5] $BiFeO_3$,[38] and Bi_2FeCrO_6,[39] also under experimental conditions where surfaces should be oxidized. To rule out that ferroelectric $LaTiO_2N$ behaves differently from other ferroelectrics such as $BaTiO_3$, we repeat our calculations for $BaTiO_3$ surfaces with differently polarized bulk structures. We find that also for $BaTiO_3$, the surface polarization direction changes with surface oxidation, leading—as for $LaTiO_2N$—to very similar densities of states at the surface (see Fig. S2 of the supplementary material).

One might further argue that the photocatalytic experiments were conducted using $BaTiO_3$ nanoparticles that are much thicker than our slabs and that the slab thickness should be increased to approach experimental conditions. As can be seen in Sec. S4 of the supplementary material, doubling the $BaTiO_3$ slab thickness does not affect the results for slabs with positive and negative bulk polarization, independent of the state of surface oxidation, even though the number of reversed layers increases. Fixing more atomic layers at bulk polarization positions (see Fig. S6 of the supplementary material), does not change the surface electronic state either. As opposed to $BaTiO_3$, we find for $LaTiO_2N$ subtle changes in the electronic structures of bulk layers as a function of the slab thickness and the number of fixed atomic layers (see Sec. S5 of the supplementary material). Nevertheless, the surface electronic properties, which should dominate the adsorption energies, also for $LaTiO_2N$ do not depend on the slab thickness and the number of fixed layers (see Secs. S5 and S6 of the supplementary material). We therefore conclude that while for both materials, the slabs used above are thick enough to reliably describe the surface properties, even thicker slabs than those shown in Secs. S4 and S5 of the supplementary material would be needed to investigate the bulk electronic structure of polar $LaTiO_2N$, which is however not of relevance in the present study that focuses on surface properties.

The reliability of our computational setup could, in principle, be further increased by including an implicit or explicit polarizable electrolyte or by adopting adsorbate coverages between the low and full coverage situations used here. While both factors should have an influence on the adsorption energies on a semiconductor surface and therefore the reaction kinetics,[20,40] we do not expect them to have a significant effect on the observed polarization reversal caused

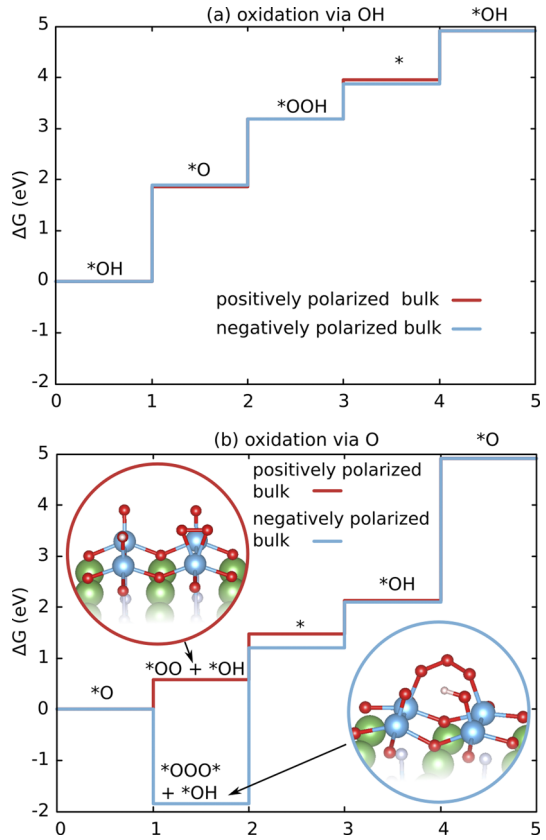

FIG. 6. Free energy profile for the OER on the *trans* $LaTiO_2N$ (001) surface with positively and negatively polarized bulk for (a) a surface oxidized with hydroxo species and (b) a surface oxidized with oxygen species. Color code: La = green, Ti = blue, O = red, N = gray, and H = white.

by electron accepting adsorbates and we can therefore neglect them for our purposes.

From our computed surface phase diagrams (see Figs. 4 and S1) and in agreement with other studies,[13,41,42] we however see that the transition potential between different types of adsorbates (clean, OH, O) slightly differs as a function of the bulk polarization. If we were to consider the large space of possible mixed and/or submonolayer adsorbate coverages, this implies that the adsorbate structure could differ significantly between surfaces with different bulk polarization. As we see by comparing Figs. 6(a) and 6(b), different adsorbates can indeed have a large effect on the overpotential of a surface, which was also reported for other materials.[20] This implies that the effect of the bulk polarization on the catalytic activity is not due to the fact that the surface is polarized in the same way as the bulk but due to the fact that the very configuration of the surface differs for differently polarized bulk domains. While this is a plausible explanation, we want to mention bulk polarization-induced surface reconstructions that deviate from our perfectly flat surfaces as another possible reason for the experimentally observed different activities. Given the plethora of possible adsorbate coverages and surface reconstructions, it is unlikely that computation alone can give definitive explanations for different catalytic activities on oxidized ferroelectric surfaces but that experimental local-probe and spectroscopic investigations are needed in conjunction with these calculations to elucidate the structure-activity relations.

IV. CONCLUSIONS

Analyzing the free energy profiles of the OER on clean surfaces with oppositely polarized bulk structures we find, in agreement with other theoretical studies, clear differences in the free energy steps for surfaces with positively and negatively polarized bulk structures. In this case, the surfaces have the same polarization direction as the bulk. However, as soon as the surface is oxidized, its polarization is positive, independent of the polarization of the underlying bulk. This results in a very similar electronic structure and hence free energy steps, independent of the bulk polarization. This disagrees with experimental studies that found different catalytic activities for differently polarized domains under conditions where surfaces should be oxidized. Based on slight differences in the surface phase diagrams for surfaces with different bulk polarization, we postulate that the origin of the experimentally observed activity difference is due to different surface adsorbate structures or surface reconstructions and not the fact that the surface is polarized in the same way as the bulk. Given the plethora of possible adsorbate configurations and reconstructions, experimental local-probe or spectroscopy studies are crucially needed in conjunction with calculations to elucidate the structure and hence the catalytic activity of oxidized ferroelectric surfaces.

SUPPLEMENTARY MATERIAL

See the supplementary material for surface phase diagrams at pH = 0, results for $BaTiO_3$ surfaces, and validation of results with respect to slab thickness and the number of fixed layers.

ACKNOWLEDGMENTS

This research was funded by the SNF Professorship (Grant No. PP00P2_157615). Calculations were performed on UBELIX (http://www.id.unibe.ch/hpc), the HPC cluster at the University of Bern, the Swiss National Supercomputing Centre (CSCS) under Project No. s766 and SuperMUC at GCS@LRZ, Germany, for which we acknowledge PRACE for awarding us access.

REFERENCES

[1]K. Garrity, A. Kakekhani, A. Kolpak, and S. Ismail-Beigi, Phys. Rev. B **88**, 045401 (2013).
[2]C. Noguera, J. Phys.: Condens. Matter **12**, R367 (2000).
[3]J. L. Giocondi and G. S. Rohrer, Chem. Mater. **13**, 241 (2001).
[4]R. Nasby and R. K. Quinn, Mater. Res. Bull. **11**, 985 (1976).
[5]J. L. Giocondi and G. S. Rohrer, J. Phys. Chem. B **105**, 8275 (2001).
[6]M. S. Marshall, A. Malashevich, A. S. Disa, M.-G. Han, H. Chen, Y. Zhu, S. Ismail-Beigi, F. J. Walker, and C. H. Ahn, Phys. Rev. Appl. **2**, 051001 (2014).
[7]A. Kakekhani and S. Ismail-Beigi, ACS Catal. **5**, 4537 (2015).
[8]A. Kakekhani, S. Ismail-Beigi, and E. I. Altman, Surf. Sci. **650**, 302 (2016).
[9]A. Logadottir, T. H. Rod, J. K. Nørskov, B. Hammer, S. Dahl, and C. Jacobsen, J. Catal. **197**, 229 (2001).

[10]J. K. Nørskov, T. Bligaard, A. Logadottir, S. Bahn, L. B. Hansen, M. Bollinger, H. Bengaard, B. Hammer, Z. Sljivancanin, M. Mavrikakis *et al.*, J. Catal. **209**, 275 (2002).
[11]I. C. Man, H.-Y. Su, F. Calle-Vallejo, H. A. Hansen, J. I. Martínez, N. G. Inoglu, J. Kitchin, T. F. Jaramillo, J. K. Nørskov, and J. Rossmeisl, ChemCatChem **3**, 1159 (2011).
[12]J. H. Lee and A. Selloni, Phys. Rev. Lett. **112**, 196102 (2014).
[13]A. Kakekhani and S. Ismail-Beigi, J. Mater. Chem. A **4**, 5235 (2016).
[14]D. Oka, Y. Hirose, H. Kamisaka, T. Fukumura, K. Sasa, S. Ishii, H. Matsuzaki, Y. Sato, Y. Ikuhara, and T. Hasegawa, Sci. Rep. **4**, 4987 (2014).
[15]D. Oka, Y. Hirose, F. Matsui, H. Kamisaka, T. Oguchi, N. Maejima, H. Nishikawa, T. Muro, K. Hayashi, and T. Hasegawa, ACS Nano **11**, 3860 (2017).
[16]N. Vonrüti and U. Aschauer, Phys. Rev. Mater. **2**, 105401 (2018).
[17]N. Vonrüti and U. Aschauer, Phys. Rev. Lett. **120**, 046001 (2018).
[18]A. Fuertes, J. Mater. Chem. **22**, 3293 (2012).
[19]A. Kasahara, K. Nukumizu, G. Hitoki, T. Takata, J. N. Kondo, M. Hara, H. Kobayashi, and K. Domen, J. Phys. Chem. A **106**, 6750 (2002).
[20]J. H. Montoya, M. Garcia-Mota, J. K. Nørskov, and A. Vojvodic, Phys. Chem. Chem. Phys. **17**, 2634 (2015).
[21]S. Wemple, Phys. Rev. B **2**, 2679 (1970).
[22]P. Giannozzi, S. Baroni, N. Bonini, M. Calandra, R. Car, C. Cavazzoni, D. Ceresoli, G. L. Chiarotti, M. Cococcioni, I. Dabo, A. Dal Corso, S. de Gironcoli, S. Fabris, G. Fratesi, R. Gebauer, U. Gerstmann, C. Gougoussis, A. Kokalj, M. Lazzeri, L. Martin-Samos, N. Marzari, F. Mauri, R. Mazzarello, S. Paolini, A. Pasquarello, L. Paulatto, C. Sbraccia, S. Scandolo, G. Sclauzero, A. P. Seitsonen, A. Smogunov, P. Umari, and R. M. Wentzcovitch, J. Phys.: Condens. Matter **21**, 395502 (2009).
[23]J. P. Perdew, K. Burke, and M. Ernzerhof, Phys. Rev. Lett. **77**, 3865 (1996).
[24]V. I. Anisimov, J. Zaanen, and O. K. Andersen, Phys. Rev. B **44**, 943 (1991).
[25]D. Vanderbilt, Phys. Rev. B **41**, 7892 (1990).
[26]S. Ninova and U. Aschauer, J. Mater. Chem. A **5**, 11040 (2017).
[27]N. Vonrüti and U. Aschauer, Phys. Chem. Chem. Phys. **21**, 24354–24360 (2019).
[28]L. Bengtsson, Phys. Rev. B **59**, 12301 (1999).
[29]H. J. Monkhorst and J. D. Pack, Phys. Rev. B **13**, 5188 (1976).
[30]K. Momma and F. Izumi, J. Appl. Crystallogr. **44**, 1272 (2011).
[31]J. K. Nørskov, J. Rossmeisl, A. Logadottir, L. Lindqvist, J. R. Kitchin, T. Bligaard, and H. Jonsson, J. Phys. Chem. B **108**, 17886 (2004).
[32]A. Valdes, Z.-W. Qu, G.-J. Kroes, J. Rossmeisl, and J. K. Nørskov, J. Phys. Chem. C **112**, 9872 (2008).
[33]R. O. Jones and O. Gunnarsson, Rev. Mod. Phys. **61**, 689 (1989).
[34]A. N. Morozovska, E. A. Eliseev, N. V. Morozovsky, and S. V. Kalinin, Phys. Rev. B **95**, 195413 (2017).
[35]R. Wang, D. Fong, F. Jiang, M. Highland, P. Fuoss, C. Thompson, A. Kolpak, J. Eastman, S. Streiffer, A. Rappe *et al.*, Phys. Rev. Lett. **102**, 047601 (2009).
[36]Y. Tian, L. Wei, Q. Zhang, H. Huang, Y. Zhang, H. Zhou, F. Ma, L. Gu, S. Meng, L.-Q. Chen *et al.*, Nat. Commun. **9**, 3809 (2018).
[37]H. Lee, T. H. Kim, J. J. Patzner, H. Lu, J.-W. Lee, H. Zhou, W. Chang, M. K. Mahanthappa, E. Y. Tsymbal, A. Gruverman *et al.*, Nano Lett. **16**, 2400 (2016).
[38]W. Ji, K. Yao, Y.-F. Lim, Y. C. Liang, and A. Suwardi, Appl. Phys. Lett. **103**, 062901 (2013).
[39]S. Li, B. AlOtaibi, W. Huang, Z. Mi, N. Serpone, R. Nechache, and F. Rosei, Small **11**, 4018 (2015).
[40]J. A. Gauthier, C. F. Dickens, L. D. Chen, A. D. Doyle, and J. K. Nørskov, J. Phys. Chem. C **121**, 11455 (2017).
[41]E. H. Morales, J. M. P. Martirez, W. A. Saidi, A. M. Rappe, and D. A. Bonnell, ACS Nano **8**, 4465 (2014).
[42]W. A. Saidi, J. M. P. Martirez, and A. M. Rappe, Nano Lett. **14**, 6711 (2014).